Electronic Supplementary Material (ESI) for Nanoscale.
This journal is © The Royal Society of Chemistry 2022

Supporting Information

Spatial homojunction of titanium vacancies decorated oxygen vacancies in TiO_2 and its directed charge transfer

*Si-Ming Wu, Yi-Tian Wang, Shi-Tian Xiao, Li-Ying Wang, Ge Tian, Jiang-Bo Chen, Jia-Wen Liu, Menny Shalom, and Xiao-Yu Yang**

Experimental Procedures

1. Materials

Tetrabutoxytitanium ($Ti(OC_4H_9)_4$, TBOT) was purchased from Aladdin. Ammonium hydroxide (25%*wt*), glycerol, ethanol and acetone were purchased from Shanghai Chemical Regent Factory of China. Distilled water was used in all experiments.

2. Preparation of np_x-TiO_2 and n-TiO_2.

As-TiO_2 was prepared by the hydrolysis of TBOT and calcination treatment according to previous work. For the synthesis of np-TiO_2, 0.2 g As-TiO_2 was dispersed in the mixture of 30 mL ethanol and 10 mL glycerol. After that, x mL of TBOT was added into the mixture while stirring. The mixture was transferred into a 100 mL Teflon-lined stainless-steel autoclave and put in an oven with 180°C for 24h. The obtained product (As-np-TiO_2) was filtrated and washed with ethanol, and then dried at 60 °C overnight. The resulting sample was calcined at 350 °C for 4 h and the heating rate to the target temperature is 1 °C/min. The obtained sample is named as np_x-TiO_2. As comparison n-TiO_2 was prepared by the same procedure without the adding of TBOT.

2. Characterization

Scanning electron microscopy (SEM) images were taken with a Hitachi S4800 electron microscope. Electron paramagnetic resonance (EPR) measurements were performed at the X-band using a JEOL FA 2000 spectrometer, with the microwave frequency of 9.163 GHz, the modulation amplitude of 0.1 mT, the microwave power of 1 mW, and the experimental temperature of 295 K. Powder X-ray diffraction (XRD) patterns were recorded by a D8 Advance X-ray diffractometer (Bruker, Germany) with Cu-Kα radiation (λ = 0.15406 nm) operated at 40 kV, 40 mA. Thermogravimetric analysis (TGA) was conducted using a NETZSCH STA 449 F3 thermogravimetric analyzer with a heating rate of 10 °C min^{-1} under air. The nitrogen adsorption and desorption isotherms of the samples were measured using a Micromeritics TriStar TM II 3020. Before the measurements, the samples were outgassed at 100 °C in vacuum for 12 h. Transmission electron microscopy (TEM) experiments were conducted on a Talos-F200S STEM/EDS electron microscope operated at 200 kV. Raman analysis was performed using a Renishaw InVia Raman spectrometer under visible excitation at 532 nm. Fourier-transform infrared (FT-IR) spectra were obtained with a Thermo Nicolet 360 spectrometer. ^1H magic-angle spinning (MAS) NMR and 2D ^1H DQ-SQ MAS NMR

spectra were carried out in a 1.9 mm MAS probe on a Bruker AVANCE-III 500 spectrometer with a sample spinning rate of 38 kHz, a ^{1}H $\pi/2$ pulse length of 1.65 μs and a recycle delay of 2 s. X-ray photoelectron spectra (XPS) of the samples were recorded on a PHI Quantera II, (ULVAC-PHI, Japan) using a monochromated Al-Kα X-ray source. Accurate binding energies (±0.1 eV) were determined with respect to the position of the adventitious C 1s peak at 284.8 eV. The photoluminescence (PL) spectra were measured by a Perkin-Elmer LS55 spectrometer with an excitation wavelength of 320 nm. Ultraviolet-visible spectroscopy diffuse reflectance spectra (UV-vis DRS) were attained using a Shimadzu UV-vis spectrophotometer (UV-2550). The spectra from 200 to 800 nm were taken at room temperature in air.

3. Photocatalytic Experiment.

In all the photocatalytic experiments described below, the light source is a 300 W xenon lamp (PLS-SXE-300D, Beijing Perfectlight Technology Co., Ltd.) with full light spectrum, and the incident light intensity at the location of photocatalysts was fixed to 100 mW/cm^2.

Photocatalytic degradation. To investigate the photocatalytic activity of the nanostructured TiO_2 samples, methylene blue (MB) and acetone were used as model pollutants for photodegradation. For MB degradation, 20 mg photocatalysts were dispersed in 100 mL aqueous solution containing 0.01 g/L MB. After stirring for 1 h in the dark until the concentration of MB remained unchanged, the reactor was then illuminated. 2 mL supernatant was taken out with an interval time of 10 min and analysed by UV-visible spectrometry (UV2550, Shimadzu, Japan). For acetone degradation, 10 mg samples were dispersed in 1 mL ethanol/water solution (1:1 v/v) and then dropped onto a dish with a diameter of ca. 3 cm. The dish was then dried at 80 °C for 12 h and then cooled to room temperature before being used. After putting the photocatalysts into the reactor, 5 μL of acetone was injected into the reactor with a micro syringe. The reactor was kept in the dark for a certain time to reach adsorption-desorption equilibrium before illumination. The analysis was conducted with a gas chromatograph (GC) (Agilent 2920B) equipped with a flame ionization detector (FID).

Photocatalytic hyrdogen production. Photocatalytic H_2 production was carried out in a closed circulation system. 20 mg of photocatalysts was dispersed in 80 mL of an aqueous solution containing 50 mL distilled H_2O, 30 mL methanol and 52 μL H_2PtCl_6 (0.01 mol/L). The mixture solution was sealed in a quartz container, and the system was vacuumed with a vacuum pump for 10 minutes to remove the dissolved oxygen, at the same time, a continuous magnetic stirrer and cooling water were applied during the experiment. The Agilent 7890 A GC with a thermal

conductivity detector (TCD) was used for analysis of the produced H_2. The simulated seawater used in photocatalytic H_2 production is 3.5 wt% NaCl aqueous solution.

4. Photoelectrochemical Measurements.

Photocurrent tests were carried out in a conventional three-electrode system using a Autolab PGSTAT302N electrochemical workstation (Metrohm, Switzerland) with a Pt foil as the counter electrode and a Ag/AgCl reference electrode. The working electrodes were prepared by dispersing catalysts (5 mg) and Nafion solution (100 μL, 0.5 wt%) in water/ethanol mixed solvent (1 mL, 1:1 v/v) at least 30 min of sonication to form a homogeneous ink. The working electrode was synthesized by drop-casting the above ink (80 μL) onto FTO glass with an area of 1 cm^2.

5. Density Functional Theory Calculations.

The DFT calculations were carried out by using the Vienna Ab initio Simulation Package (VASP). The exchange-correlation interaction was described by generalized gradient approximation (GGA) with the Perdew–Burke–Ernzerhof (PBE) functional. The Brillouin zone was integrated with a Monkhorst–Pack 3×3×1 k-point grid and plane-wave energy cutoff of 520 eV for all calculations. Anatase (001) surfaces with O vacancy and Ti vacancy were built to form heterogeneous interface. Van der Waals (vdW) correction was adopted to describe long-range vdW interactions and dipole-dipole interaction was employed due to the asymmetric layercluster arrangement. The convergence criteria for energy and force were 10^{-5} eV and 0.02 eV/Å, respectively.

Results and Discussion

Table S1. The BET surface area, pore volume and pore diameter of n-TiO_2 and np-TiO_2.

Samples	S_{BET} [m^2 g^{-1}]	Pore volume [cm^3 g^{-1}]	Pore Diameter [nm]
n-TiO_2	79	0.09	3.1
np-TiO_2	59	0.08	2.2

Table S2. Parameters of equivalent circuits for the impedance data of n-TiO_2 and np-TiO_2.

Samples	R_{ct} (Ω)	R_s (Ω)	CPE ($\times 10^{-5}\Omega^{-1}$)
n-TiO_2	7445	128	8.4
np-TiO_2	1820	118	6.6

Table S3. Summary of the TiO_2-based materials in photocatalytic water splitting.

Photocatalyst	Light source	H_2 production rate (mmol h^{-1} g^{-1})	System	Ref.
0.5 wt% Pt/TiO_2	300 W Xe lamp	26.4	Water/Methanol	Our work
0.5 wt% Pt/TiO_2	300 W Xe lamp	8.6	Water/Methanol	[1] (Nanoscale 2020)
0.5 wt% Pt/TiO_2	300 W Xe lamp	9.26	Water/Methanol	[2] (ACS Catal. 2019)
0.6 wt% Pt/TiO_2	300 W Xe lamp	8.45	Water/Methanol	[3] (J. Catal. 2017)
1.0 wt% Pt/TiO_2	100 W Hg lamp	1.441	Water/Methanol	[4] (Adv. Mater. 2019)
1.0 wt% Pt/TiO_2	300 W Xe lamp	5.827	Water/Methanol	[5] (Energy Environ. Sci. 2018)

Table S4. Corrosion potential of the bare 304 SS and 304 SS coupled with different electrodes in 3.5 wt% NaCl solution under illumination.

Samples	E_{corr} (mV vs. Ag/AgCl)
304 SS	-210
n-TiO_2	-309
np-TiO_2	-327
np_{mix}-TiO_2	-280

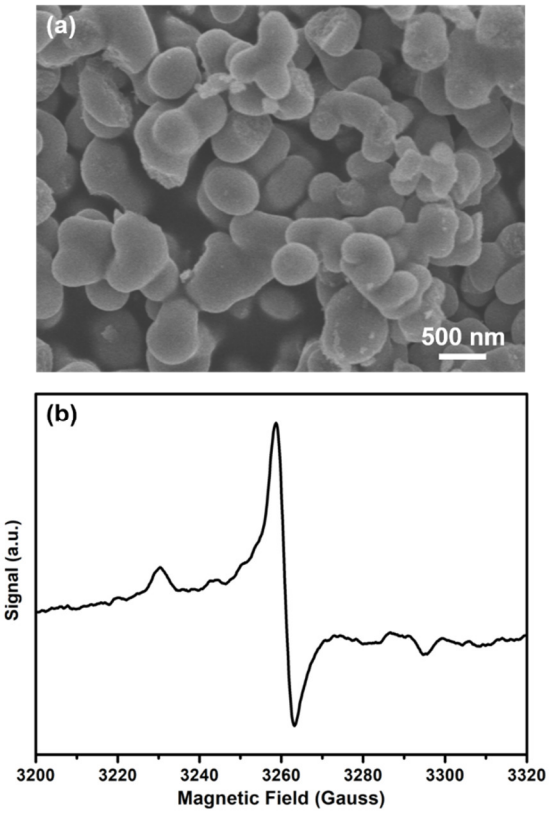

Figure S1. (a) SEM image of As-TiO_2, (b) EPR spectrum of As-TiO_2.

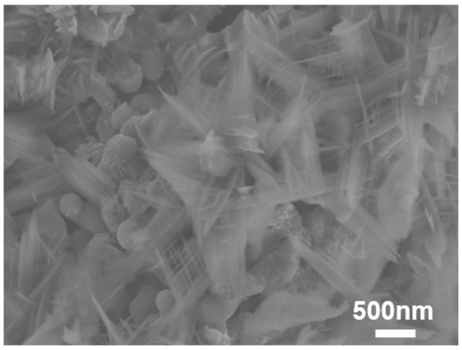

Figure S2. SEM image of As-np-TiO_2.

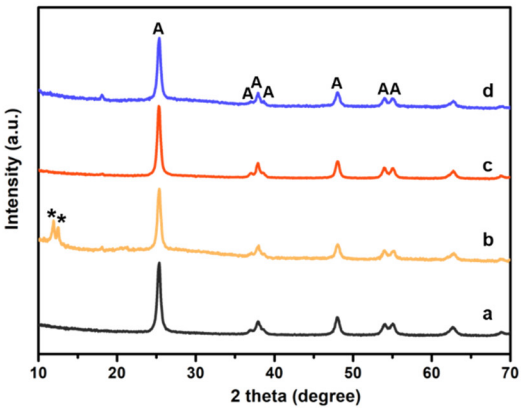

Figure S3. XRD patterns of a. As-TiO_2, b, As-np-TiO_2, c. np-TiO_2, d. n-TiO_2. A refers to anatase phase of TiO_2, * refers to titanium glycerolate.

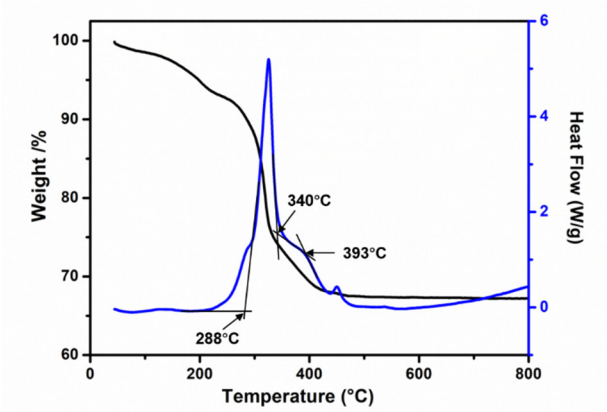

Figure S4. TG and DTA curves of As-np-TiO_2. The weight loss of the TiO_2-A before 288 °C is around 20%, which is due to the loss of absorption of water and possible hydrolysate residues of tetrabutyl titanate. 288 °C is the starting temperature for partial phase transformation of sol-gel TiO_2 from the amorphous phase to metastable anatase phase. The free energy of the anatase transformation is negative at least above 400 °C, which is full phase-transformation from the amorphous phase to anatase phase.

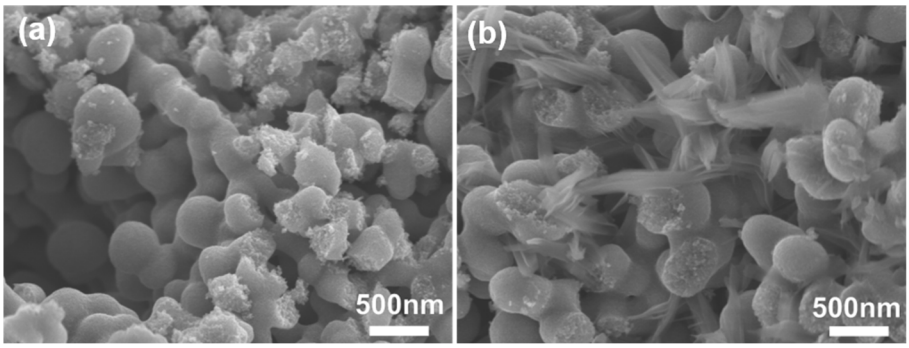

Figure S5. SEM images of (a) n-TiO_2 and (b) np-TiO_2.

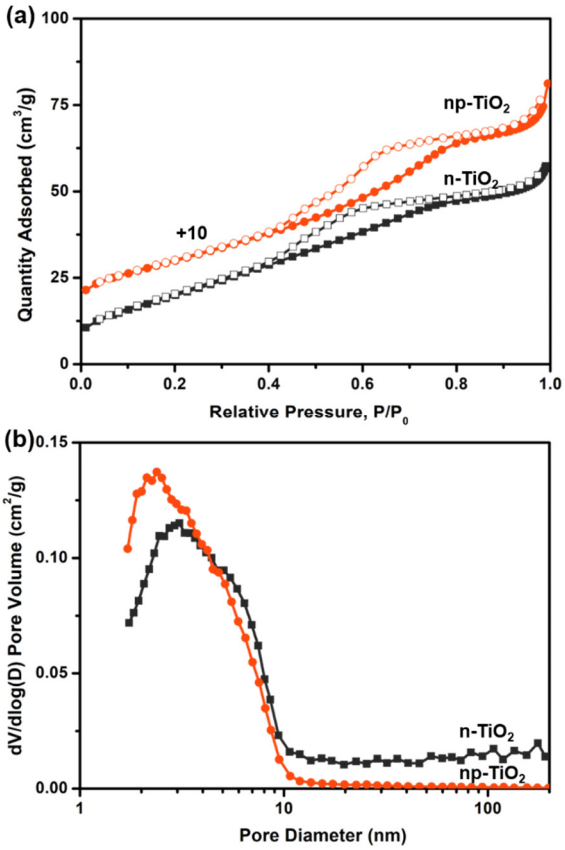

Figure S6. (a) Nitrogen-adsorption-desorption isotherms and (b) corresponding pore size distribution of n-TiO_2 and np-TiO_2.

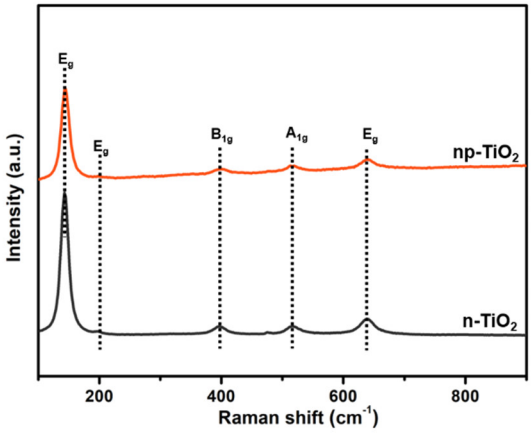

Figure S7. Raman spectra of n-TiO_2 and np-TiO_2. Five peaks at 143, 195, 395, 515, and 638 cm^{-1} could be belonged to typical anatase Raman bands of Eg, Eg, B1g, A1g(B1g), and Eg modes, respectively.[3]

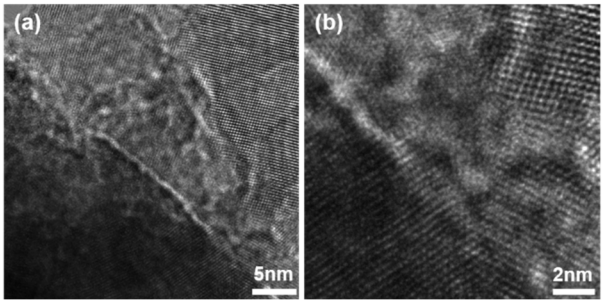

Figure S8. (a) Origin TEM image of Figure 1f, (b) Origin TEM image of Figure 1g.

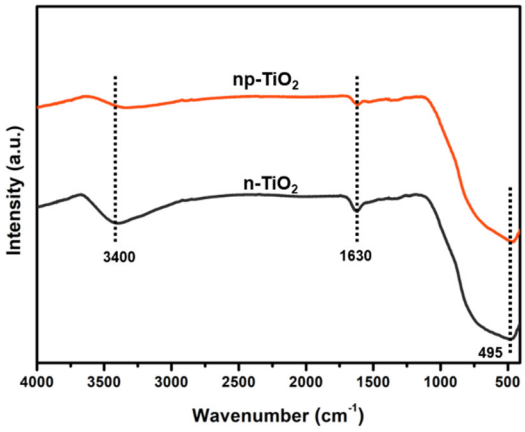

Figure S9. FT-IR spectra of of n-TiO_2 and np-TiO_2.

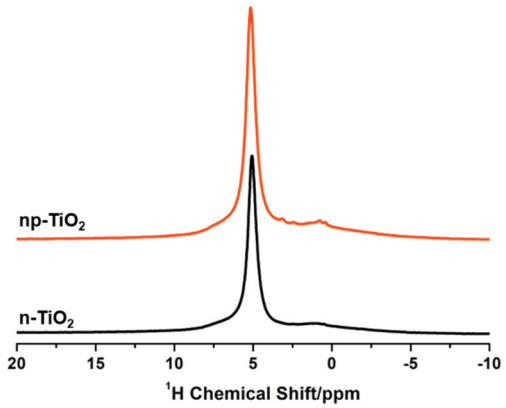

Figure S10. ^{1}H NMR spectra of of n-TiO_2 and np-TiO_2.

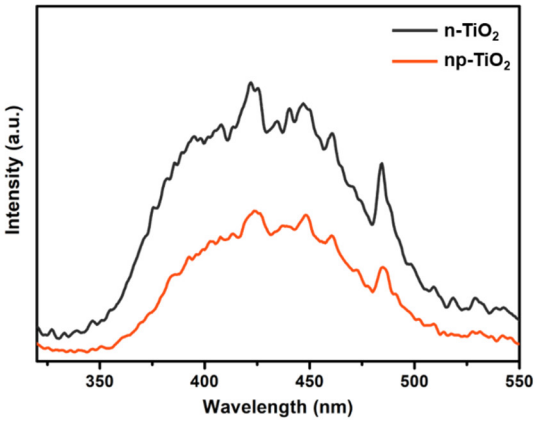

Figure S11. PL spectra of n-TiO_2 and np-TiO_2.

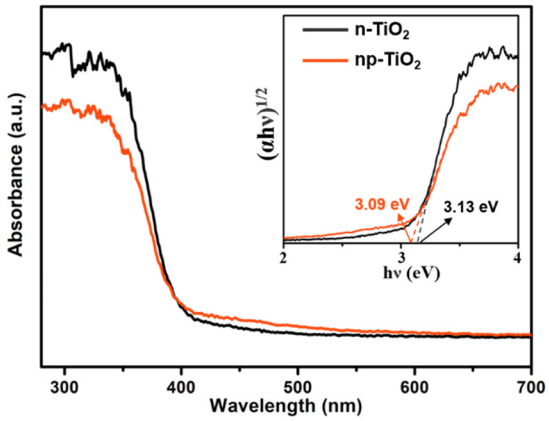

Figure S12. UV-vis diffuse reflectance spectra of n-TiO_2 and np-TiO_2. The inset is curves of Kubelka-Munk function as the vertical axis and plotted against the photon energy.

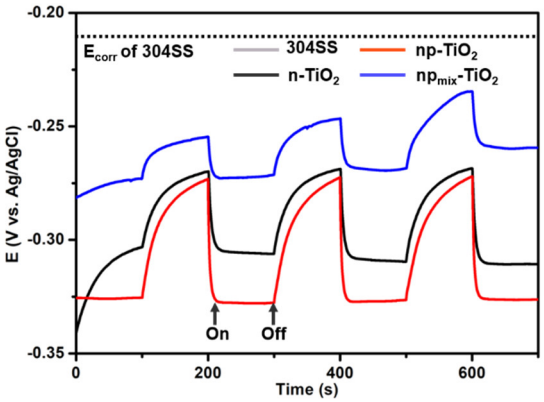

Figure S13. OCP variations of 304SS coupled with n-TiO_2, np-TiO_2, and np_{mix}-TiO_2 electrodes in 3.5 wt% NaCl solution with intermittent illumination.

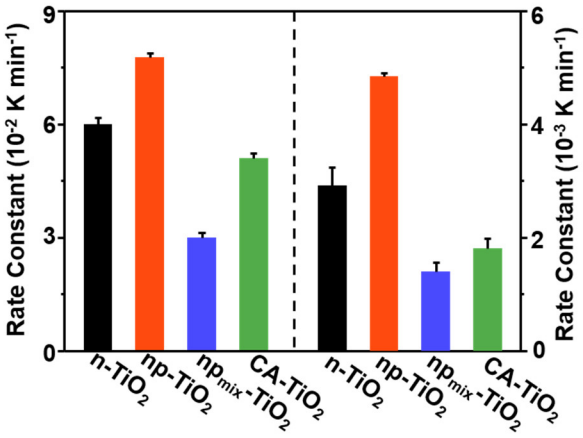

Figure S14. Photocatalytic rate constants for degradations of methylene blue (MB) and acetone with different samples under UV-Vis light irradiation.

Reference

[1] Y. Lu, Y. X. Liu, L. He, L.-Y. Wang, X. L. Liu, J. W. Liu, Y. Z. Li, G. Tian, H. Zhao, X. H. Yang, J. Liu, C. Janiak, S. Lenaerts, X.-Y. Yang, B.-L. Su, *Nanoscale,* 2020, **12**, 8364-8370

[2] Y. Bai, Y. E. Zhou, J. Zhang, X. B. Chen, Y. H. Zhang, J. F. Liu, J. Wang, F. F. Wang, C. D. Chen, C. Li, R. G. Li, C. Li, *ACS Catal.* 2019, **9,** 3242-3252.

[3] Y. L. Sui, S. B. Liu, T. F. Li, Q. X. Liu, T. Jiang, Y. F. Guo, J. L. Luo, *J. Catal.* 2017, **353**, 250-255.

[4] C. M. Gao, Tao. Wei, Y. Y. Zhang, X. H. Song, Y. Huan, H. Liu, M. W. Zhao, J. H. Yu, X. D. Chen, *Adv. Mater.* 2019, **31**, 1806596.

[5] A.-Y. Zhang, W. Y. Wang, J.-J. Chen, C. Liu, Q. X. Li, X. Zhang, W. W. Li, Y. Si, H. Q. Yu, *Energy Environ. Sci.* 2018, **11**, 1444-1448.

.